

Article

Cold adaptation in pigs depends on UCP3 in beige adipocytes

Jun Lin^{1,2,†}, Chunwei Cao^{3,†}, Cong Tao^{4,†}, Rongcai Ye^{1,2}, Meng Dong^{1,2}, Qiantao Zheng^{2,3}, Chao Wang⁴, Xiaoxiao Jiang^{1,2}, Guosong Qin³, Changguo Yan⁵, Kui Li⁴, John R. Speakman⁶, Yanfang Wang^{4,*}, Wanzhu Jin^{1,7,*}, and Jianguo Zhao^{3,7,*}

¹ Key Laboratory of Animal Ecology and Conservation Biology, Institute of Zoology, Chinese Academy of Sciences, Beijing 100101, China

² College of Life Science, University of Chinese Academy of Sciences, Beijing 100049, China

³ State Key Laboratory of Stem Cell and Reproductive Biology, Chinese Academy of Sciences, Beijing 100101, China

⁴ State Key Laboratory of Animal Nutrition, Institute of Animal Science, Chinese Academy of Agricultural Sciences, Beijing 100193, China

⁵ Department of Animal Science, Yanbian University, Yanji 133002, China

⁶ State Key Laboratory of Molecular Developmental Biology, Institute of Genetics and Developmental Biology, Chinese Academy of Sciences, Beijing 100101, China

⁷ Savaid Medical School, University of Chinese Academy of Sciences, Beijing 100049, China

[†] These authors contributed equally to this work.

* Correspondence to: Yanfang Wang, E-mail: Wangyanfang@caas.cn; Wanzhu Jin, E-mail: Jinw@ioz.ac.cn; Jianguo Zhao, E-mail: zhaojg@ioz.ac.cn

Pigs lack functional uncoupling protein 1 (UCP1) making them susceptible to cold. Nevertheless, several pig breeds are known to be cold resistant. The molecular mechanism(s) enabling such adaptation are currently unknown. Here, we show that this resistance is not dependent on shivering, but rather depends on UCP3 and white adipose tissue (WAT) browning. In two cold-resistant breeds (Tibetan and Min), but not a cold-sensitive breed (Bama), WAT browning was induced after cold exposure. Beige adipocytes from Tibetan pigs exhibited greater oxidative capacity than those from Bama pigs. Notably, UCP3 expression was significantly increased only in cold-resistant breeds, and knockdown of UCP3 expression in Tibetan adipocytes phenocopied Bama adipocytes in culture. Moreover, the eight dominant pig breeds found across China can be classified into cold-sensitive and cold-resistant breeds based on the UCP3 cDNA sequence. This study indicates that UCP3 has contributed to the evolution of cold resistance in the pig and overturns the orthodoxy that UCP1 is the only thermogenic uncoupling protein.

Keywords: cold resistant, brown adipose tissue, beige adipocyte, Tibetan pig, thermogenesis

Introduction

In contrast to white adipose tissue (WAT), which is the primary energy storage organ, brown adipose tissue (BAT) is specialized to produce heat via the activation of uncoupling protein 1 (UCP1). This protein embedded in the inner mitochondrial membrane converts the mitochondrial proton-motive force into heat instead of adenosine triphosphate (Klingenspor et al., 2008) and contributes to the maintenance of core body temperature (Klingenberg, 2010; Divakaruni and Brand, 2011; Dempersmier et al., 2015). In addition, the third type of fat cell termed the brown in white (brite) or beige adipocyte (hereafter referred to as beige) has been reported, which also expresses UCP1 and has thermogenic, fat-burning properties (Ishibashi and Seale, 2010; Shabalina et al., 2013; Keipert and Jastroch, 2014). The contribution of these beige cells to total thermogenic heat

production is disputed (Schulz et al., 2013; Keipert and Jastroch, 2014). There have been several other UCPs discovered over the past 20 years, which show different tissue distributions (Jezek and Garlid, 1998; Sokolova and Sokolov, 2005; Alan et al., 2009). The functions of these UCPs have been heavily debated, including whether they actually possess any uncoupling capacity and hence whether they are appropriately named (Harper et al., 2002; Schrauwen and Hesselink, 2002; Shabalina et al., 2010). Studies of the UCP1^{-/-} mice indicate that they can survive progressive exposure to lowered ambient temperatures (Ukropec et al., 2006), but this ability is dependent upon extensive and prolonged shivering (Cannon and Nedergaard, 2004). On this basis, it has been claimed that the other UCPs do not have any thermogenic capacities (Golozoubova et al., 2001; Cannon and Nedergaard, 2010).

Pigs (Suidae) have a predominantly tropical distribution and lost functional UCP1 in a genetic event that eliminated exons 3–5 ~20 million years ago (Berg et al., 2006). They consequently have also been suggested to lack functional BAT. This has some

Received January 19, 2017. Revised February 27, 2017. Accepted May 7, 2017.

© The Author (2017). Published by Oxford University Press on behalf of *Journal of Molecular Cell Biology*, IBCB, SIBS, CAS. All rights reserved.

practical implications in that it results in modern pig breeds being cold sensitive, which is a major cause of neonatal death in the swine industry (Berg et al., 2006). However, whether BAT exists in piglets is the subject of an ongoing debate (Jastroch and Andersson, 2015). It has been reported that BAT is present in the piglet based on immunohistochemical (Meister et al., 1988) and morphological analyses (Attig et al., 2008). Another study reported that porcine UCP1 is detectable by immunoblotting and gene expression analyses, suggesting its existence in pigs (Mostyn et al., 2014). In contrast, previous studies demonstrated that functional BAT was not present in the pig due to undetectable level of UCP1 protein in any tissue, regardless of age or ambient temperature (Trayhurn et al., 1989). This led to the suggestion that body temperature regulation in the piglet does not rely on BAT-derived non-shivering thermogenesis (NST) but is primarily dependent on shivering thermogenesis from the skeletal muscle (Symonds and Lomax, 1992).

Despite these inconsistent findings, some pig breeds, such as the Tibetan pig found on the Qinghai-Tibetan plateau and the Min pig living in Northeast China, are well recognized to be cold resistant (Li et al., 2013). However, the exact metabolic mechanisms by which these pigs have adapted to the cold environment and the underlying genetic basis are currently unknown. These phenotypical differences among various pig breeds raise the question whether such cold tolerance is dependent on extensive shivering, as observed in the UCP^{-/-} mice, or the BAT/UCP1-independent non-shivering thermoregulation mechanisms are involved in the thermoregulation of some pig breeds.

Here, we show that cold-tolerant pigs can thermoregulate when the ability to shiver and skeletal muscle NST are blocked, and that WAT browning (the emergence of beige adipocytes) and elevated UCP3 expression are responsible for body temperature regulation in cold-adapted pigs, such as Tibetan and Min pigs. This thermogenic mechanism has allowed them to survive in cold environments independent of BAT or UCP1 and challenges the suggestion based on studies of small rodents that

UCP1 can be the only source of significant non-shivering thermogenic heat production.

Results

Tibetan pigs lack functional BAT

To explore whether classical BAT exists in the Tibetan pig, subcutaneous WAT (sWAT), perirenal adipose tissue, and neck adipose tissue from 1-week-old newborn Tibetan piglets were collected and subjected to histological analysis. Mouse classical interscapular BAT was used as a positive control. No BAT-like adipocytes could be found in the adipose tissues of these Tibetan piglets (Figure 1A). To examine whether UCP1 is expressed in the adipose tissue of Tibetan pigs, we designed primers around exons 1–2 and 6 of the UCP1 gene in the pig genome (Supplementary Table S1) and performed reverse transcriptase-polymerase chain reaction (RT-PCR) amplification. Our results showed that no positive PCR production was detected in adipose tissues of Tibetan pigs (data not shown). Taken together, neither classical BAT nor UCP1 expression was observed in neonatal Tibetan piglets.

Tibetan pigs have an alternative mechanism to maintain body temperature different from skeletal muscle-mediated shivering thermogenesis

To further investigate the potential mechanisms underpinning the thermoregulatory ability of Tibetan pigs in cold environments, cold challenge experiments were performed, involving the administration of muscle-specific thermogenic inhibitors curare and dantrolene. The Bama miniature pig, a well-known cold-sensitive pig breed that has a similar body size to the Tibetan pig, was used as a control. Curare is a muscle-shivering inhibitor that can competitively block the binding of the neurotransmitter acetylcholine to its receptors (Bowman, 2006). We showed that without drug treatment, both Bama and Tibetan pigs showed normal shivering and maintained an average core body temperature of ~38°C during a cold challenge (Figure 1B and C).

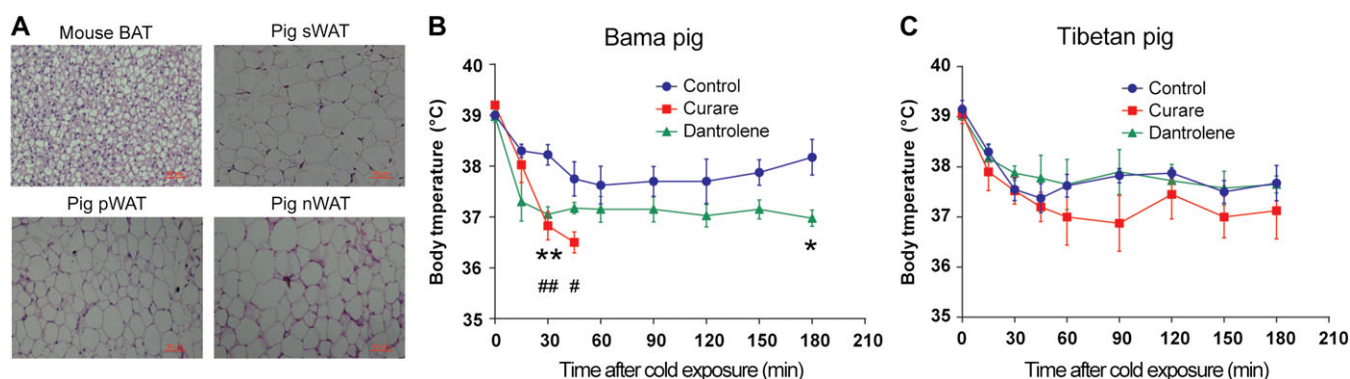


Figure 1 Tibetan pigs lack classic BAT but have a compensatory pathway in the absence of muscle thermogenesis. (A) H&E staining of tissue sections of BAT from mice and sWAT, perirenal WAT (pWAT), and neck WAT (nWAT) fat from Tibetan pigs. Note that morphologically, there is no classic BAT in these porcine fat tissues. (B and C) Core body temperature during acute cold exposure after the administration of curare or dantrolene in Bama pigs (B) and Tibetan pigs (C). Values are shown as mean \pm SEM ($n = 5$). ** $P < 0.01$, * $P < 0.05$; data were analyzed with a two-sample t -test.

Interestingly, a rapid and striking decline in core body temperature caused by curare administration was only observed in Bama pigs during the cold challenge (Figure 1B). These Bama piglets all developed severe hypothermia by 45 min after cold exposure (Figure 1B). In contrast, curare-treated Tibetan pigs showed a small, non-significant reduction in core body temperature during the cold challenge (Figure 1C), indicating that, despite lacking BAT and functional UCP1, they were able to generate heat through non-shivering mechanisms.

Previous studies have suggested that sarcolipin (Sln)-mediated NST in skeletal muscle is a potentially important mechanism for thermoregulation in mammals (Bal et al., 2012). To evaluate the contribution of muscle NST in pig thermoregulation, dantrolene, a drug that inhibits the ryanodine receptor (Ryr1)-mediated Ca^{2+} leak, which is essential for stimulating NST through the SERCA pump (Wang et al., 2011), was administered to Bama and Tibetan pigs prior to the cold challenge. Dantrolene-treated Bama pigs showed a significant decrease in their core body temperature 30–180 min after cold challenge (Figure 1B). In contrast, dantrolene injection had no significant effect on core body temperature in Tibetan pigs (Figure 1C). These results suggest that, in contrast to Bama pigs, Tibetan pigs might have an alternative pathway to maintain body temperature in cold environments in the absence of both muscle-derived shivering and NST.

Beige adipocytes are found in Tibetan pigs after cold exposure

BAT exhibits a high rate of ^{18}F -fluorodeoxyglucose (^{18}F -FDG) uptake (Cypess et al., 2009; Virtanen et al., 2009), which could be identified by positron-emission tomography (PET). To investigate whether Bama and Tibetan piglets had significant differences in ^{18}F -FDG uptake during cold exposure, ^{18}F -FDG was injected into the ear vein of piglets both at room temperature and during cold exposure, followed by a PET scan of the pigs. Our data showed that no positive PET signals were observed in either pig breed at room temperature. Notably, high ^{18}F -FDG uptake was detected in the perirenal fat, axillary sWAT, and inguinal sWAT of Tibetan pigs, but not Bama pigs, after 4 h cold exposure (Figure 2A). Histological analysis revealed that the PET-positive sWAT (Figure 2B) and perirenal fat tissue (Supplementary Figure S1A) from cold-treated Tibetan pigs clearly showed the characteristic multi-locular lipid droplets of beige cells, in contrast to the tissues from cold-treated Bama pigs (Figure 2B and Supplementary Figure S1A).

Next, sWAT from Bama and Tibetan piglets before and after cold treatment was subjected to scanning electron microscopy. The results confirmed that beige cells showing multi-locular droplet structures were only found in cold-treated Tibetan pigs (Figure 2C). It has been demonstrated that, similar to classic brown adipocytes, beige cells are enriched in mitochondria (Cannon and Nedergaard, 2004; Oelkrug et al., 2015). Consistently, transmission electron microscope (TEM) analysis revealed an increased mitochondrial copy number in the sWAT (Figure 2D) and perirenal fat tissue (Supplementary Figure S1B) of Tibetan pigs after cold exposure, which was further confirmed by quantitative real-time PCR

(Figure 2E). In addition, mitochondrial OXPHOS protein, CD137, a beige cell surface marker (Wu et al., 2012), and PPAR γ co-activator 1 α (PGC-1 α), a marker of mitochondrial biogenesis (Puigserver et al., 1998), appear to be increased largely in the sWAT of Tibetan pigs, but not Bama pigs, after cold exposure (Figure 2F). Taken together, these results provided strong evidence supporting that cold stimulation induces beige fat formation in the sWAT of Tibetan pigs.

Beige adipocytes from Tibetan pigs exhibit an elevated oxidative capacity

To further investigate the function of beige adipocytes from Tibetan pigs *in vitro*, we isolated primary pre-adipocytes from the sWAT of Tibetan pigs and induced WAT and beige adipocyte differentiation (browning effect) (Supplementary Figure S2A). BAT markers (*Dio2*, *Pgc1a*, and *Cidea*) were significantly upregulated, while WAT markers (*Rb1* and *Tcf21*) were markedly downregulated in differentiated beige adipocytes, compared with fully differentiated white adipocytes (Supplementary Figure S2B). Furthermore, mitochondrial OXPHOS protein and two transcriptional factors, *Pgc1 α* and *Prdm16*, which are required for the switch from WAT to beige cells (Cohen et al., 2014), were found to be abundant in differentiated beige cells (Supplementary Figure S2C). Moreover, *in vitro* cellular metabolic results revealed a significantly higher oxidative capacity in beige adipocytes than that in white adipocytes (Supplementary Figure S2D and E). These findings indicate that porcine primary pre-adipocytes from Tibetan pigs could be differentiated into either white or beige adipocytes.

We then isolated primary pre-adipocytes from Tibetan and Bama pigs and differentiated them into beige cells. Despite similar differentiation efficiencies in both pig lineages (Figure 3A), the expression of BAT markers (*Dio2* and *Cidea*) and beige adipocyte markers (*Slc27a1* and *Tmem26*) was significantly higher in beige adipocytes from Tibetan pigs than those from Bama pigs. Conversely, the expression of the WAT marker (*Tcf21*) was higher in Bama pigs (Figure 3B). Consistently, the expression of mitochondrial OXPHOS protein, PGC-1 α , *Dio2*, and *Prdm16* appears to be higher in Tibetan pigs than Bama pigs (Figure 3C). The calculated basal respiration, maximal respiration, and proton leakage were all higher in beige cells from Tibetan pigs than those from Bama pigs (Figure 3D and E). These results indicate that beige adipocytes from Tibetan pigs exhibit higher thermogenic capacity than those from Bama pigs.

Transcriptome analysis of the PET-positive fat

To determine the molecular signature of the response of sWAT upon acute cold exposure in both Tibetan and Bama pigs, genome-wide RNA-seq analysis was performed to identify the transcriptional profiles. The differentially expressed genes (DEGs) upon cold stimulation in Tibetan and Bama pigs were screened based on the criteria of false discovery rate (FDR) <0.05. The volcano plots, which were built based on FDR values and fold changes, showed a broad overview of the changes in gene expression of Tibetan pigs (Figure 4A) and Bama pigs (Figure 4B) during cold exposure. Clearly, a strong transcriptional response was observed in the sWAT of cold-treated

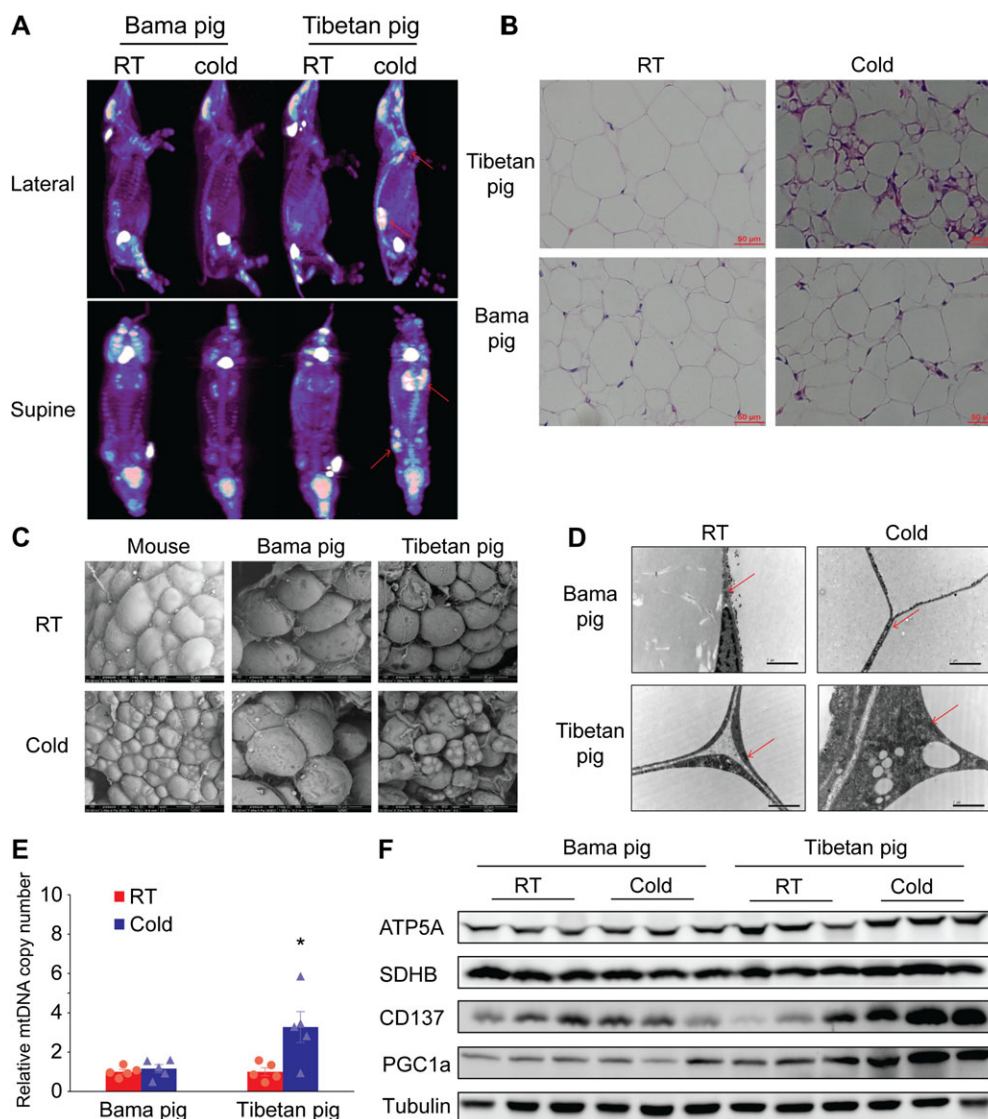


Figure 2 Tibetan pigs exhibit cold-induced beige-like adipocytes. (A) PET-positive signals were found in Tibetan pigs during cold exposure (red arrows). RT, room temperature; Cold, cold exposure for 4 h. (B–F) Representative H&E staining (B), scanning electron micrographs (C), transmission electron micrographs (D), copy number of mitochondria (E), and protein expression of mitochondrial OXPHOS and CD137 (F) for the PET-positive subcutaneous fat from Bama pigs and Tibetan pigs under RT and cold conditions. Data are presented as mean \pm SEM ($n = 5$). * $P < 0.05$; data were analyzed with a two-sample t -test.

Tibetan pigs, which was muted in Bama pig, as 230 genes exhibited significantly altered expression levels (Supplementary Table S3). In contrast, only 165 genes were differentially expressed in the sWAT of Bama pigs during cold exposure (Supplementary Table S4). Interestingly, only 28 of the DEGs overlapped between the two breeds (Supplementary Figure S3 and Table S5), suggesting that different molecular networks were involved in the responses of sWAT to cold exposure in these two pig lineages. Heat maps of gene expression revealed that the DEGs could be classified into the room temperature and cold exposure groups in both Tibetan pigs (Supplementary Figure S4A) and Bama pigs (Supplementary Figure S4B). Gene ontology (GO) analysis was performed with the DEGs in the

repressed and induced subgroups for both Tibetan and Bama pigs. Notably, the genes that were significantly induced upon cold stimulation in Tibetan pigs were enriched in GO annotations of lipid metabolic process, cellular lipid metabolic process, response to lipid and fatty acid metabolic processes, etc. (Supplementary Figure S4A). In contrast, the upregulated genes in Bama pigs were annotated as being involved in the immune response and response to external stimuli (Supplementary Figure S4B).

Importantly, UCP3, a protein that belongs to the UCP family, was dramatically increased in Tibetan pigs, but not in Bama pigs, after cold exposure. This was further confirmed by quantitative real-time PCR analysis (Figure 4C) and immunoblotting

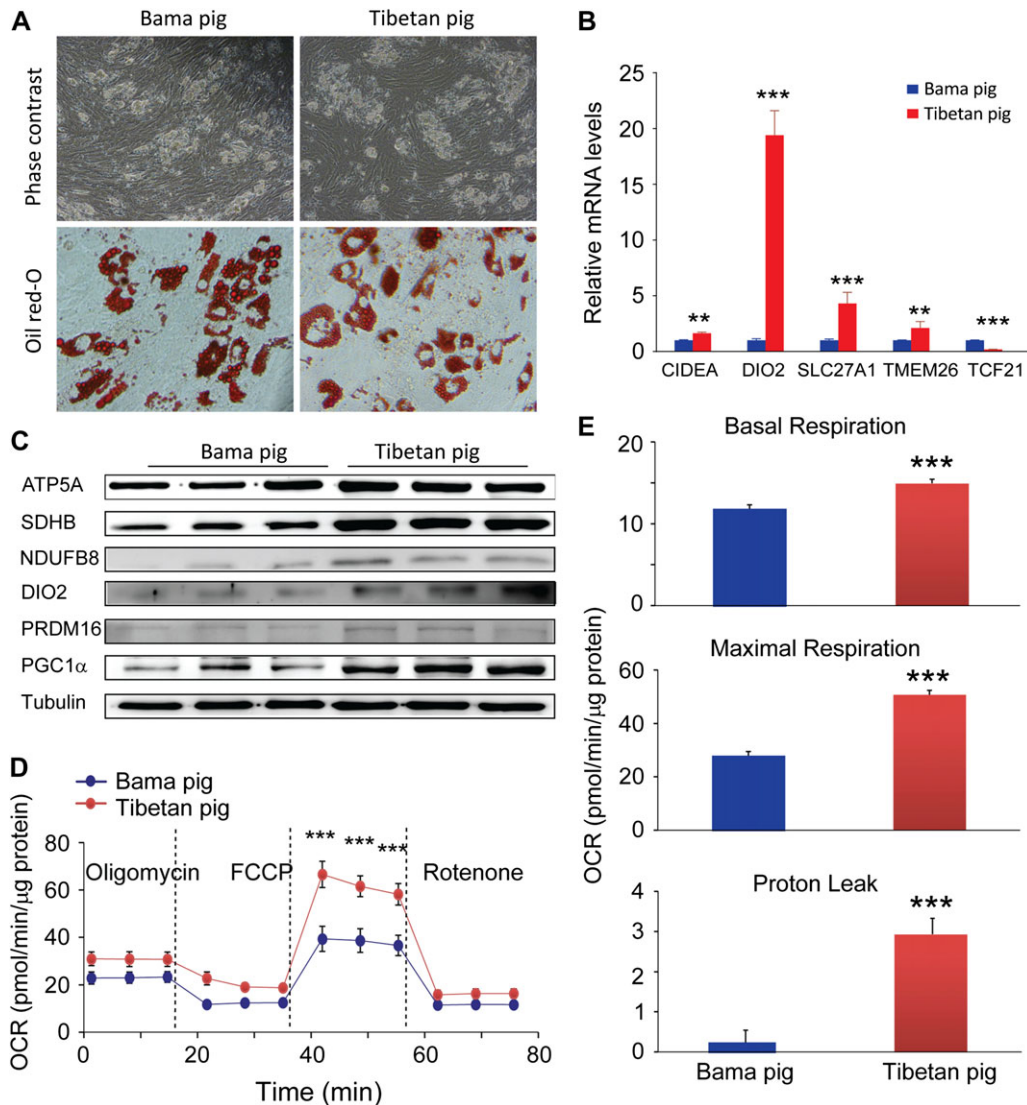


Figure 3 Differentiated beige cells derived from the subcutaneous fat of Tibetan pigs exhibit profound oxidative capacity. (A) Porcine preadipocytes can be efficiently differentiated into mature beige cells *in vitro*. Representative Oil-Red-O staining of differentiated beige adipocytes from Bama pigs and Tibetan pigs. (B–D) mRNA expression levels of BAT, beige, and WAT markers (B), protein expression levels of mitochondrial OXPHOS and BAT/beige markers (C), and the oxygen consumption rate (OCR) (D) in differentiated beige adipocytes from Bama pigs and Tibetan pigs. (E) Basal cellular respiration, maximal respiration, and proton leakage were calculated. Values are shown as mean \pm SEM ($n = 10$). *** $P < 0.001$, ** $P < 0.01$, * $P < 0.05$; data were analyzed with a two-sample *t*-test.

analysis (Figure 4D). Consistently, UCP3 was also observed to be significantly upregulated in beige cells derived from Tibetan pigs at both mRNA level (Figure 4E) and protein level (Figure 4F).

A previous report has shown that alterations in residues Gly77, Gly175, Glu261, Phe266, Lys268, and Gly269 of UCP1 can lead to a significant impairment in the regulation of the proton translocating activity of UCP1 (Gonzalez-Barroso et al., 1999). As shown in Supplementary Figure S5A, these residues were identified to be highly conserved between rodent UCP1 and porcine UCP3, suggesting that UCP3 in cold-tolerant pigs might have uncoupling activity similar to UCP1. To explore

whether the upregulation of UCP3 was involved in the thermogenesis of beige adipocytes from Tibetan pigs, we overexpressed (Supplementary Figure S5B) or knocked down (Supplementary Figure S5C) UCP3 in primary adipocytes derived from Tibetan pigs, and the fully differentiated cells were subjected to *in vitro* metabolic analysis on the Seahorse XF Analyzers. As expected, UCP3 overexpression led to a significant augmentation of cellular oxidative capacity, whereas UCP3 knockdown had the opposite effect (Figure 4G and H). These results made us speculate that UCP3 might be an important mediator of thermogenesis in cold-tolerant pigs when UCP1 is absent. Taken together, these observations indicate that the

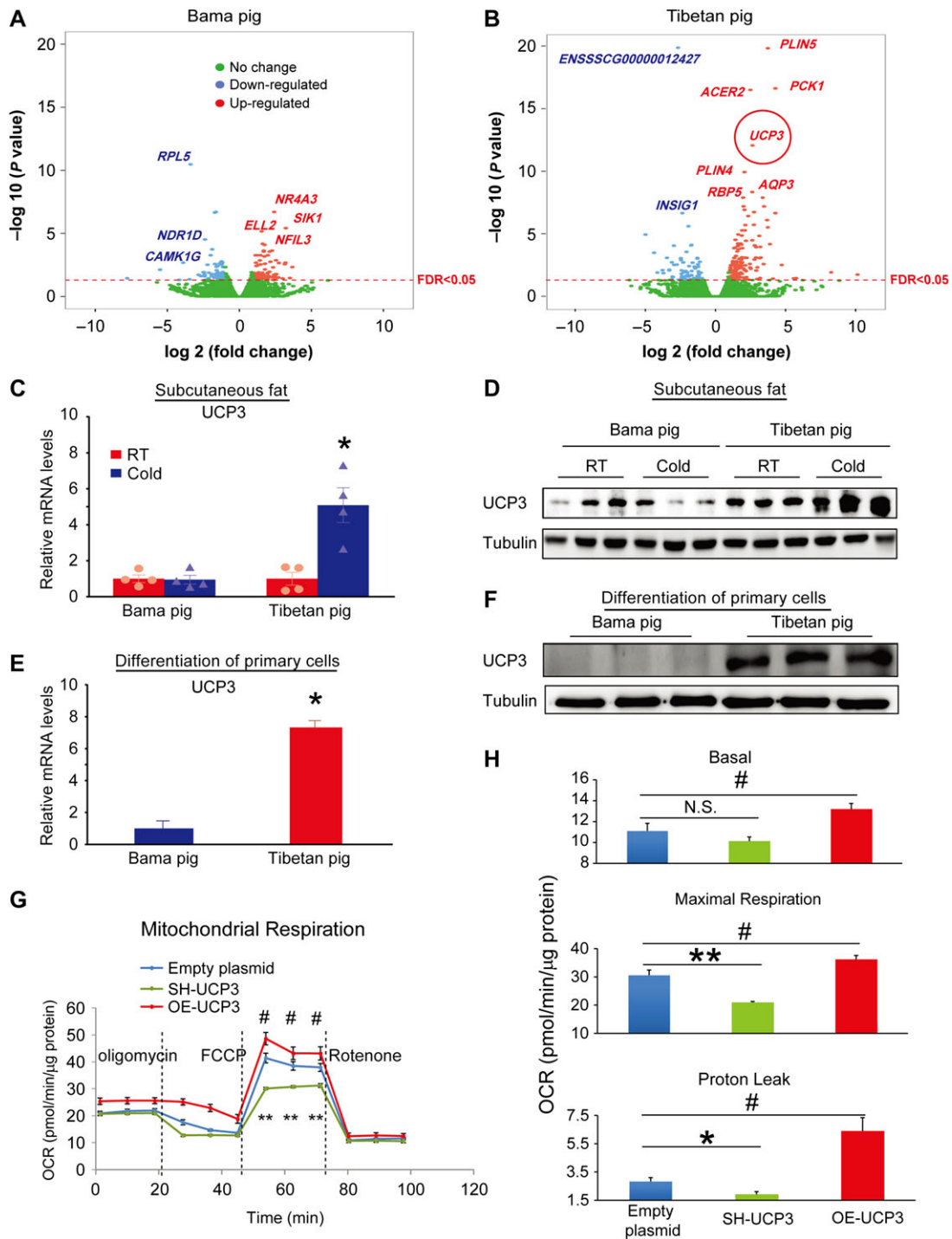


Figure 4 UCP3 plays an important role in uncoupling thermogenesis in beige adipocytes from Tibetan pigs. **(A and B)** Transcriptome analysis revealed different gene expression profiles under RT and cold conditions in Tibetan pigs **(A)** and Bama pigs **(B)**. The volcano plots show significance on the y-axis ($-\log_{10}(P)$) against the gene expression ratio (\log_2 , fold change), and the FDR cutoff <0.05 is indicated by red dashed horizontal lines. The top 10 DEGs were highlighted with their names. **(C and D)** Expression of UCP3 in subcutaneous fat from Bama pigs and Tibetan pigs under RT and cold conditions at mRNA level **(C)** and protein level **(D)**. **(E and F)** Expression of UCP3 at mRNA level **(E)** and protein level **(F)** in differentiated beige adipocytes from Bama pigs and Tibetan pigs. **(G)** OCR in differentiated beige adipocytes derived from Tibetan pigs transfected with UCP3 overexpression vector (OE-UCP3), shRNA vector targeting UCP3 (SH-UCP3), or empty vector control. **(H)** Basal cellular respiration, maximal respiration, and proton leakage were calculated. Values are shown as mean \pm SEM ($n = 5$). *** $P < 0.001$, ** $P < 0.01$, * $P < 0.05$; data were analyzed with an unpaired t -test.

distinct transcriptional responses of sWAT to cold stimulation underpin the different thermoregulatory mechanisms in Tibetan and Bama pigs.

UCP3-dependent thermogenesis in beige adipocytes is a key evolutionary response in cold-adapted pig lineages

Several pig breeds are cold tolerant. A question, therefore, is whether UCP3-dependent thermogenesis in beige cells plays a role in the evolution of cold-adapted pig breeds. To answer this question, we extended our investigations to more pig breeds, including those from the extremely cold areas of north and

northeast China and from southern tropical mainland China (Figure 5A). A neighbor joining phylogenetic tree was generated based on the multiple coding sequence alignments of the *UCP3* gene in nine different pig breeds using MEGA4 software with the default settings (Figure 5B). The three pig breeds that are distributed in cold environments, including the Min pig (MP), Tibetan pig (TP), and Hetao pig (HTP), were grouped together, whereas the other cold-sensitive pig breeds were allocated to different clusters (Figure 5B). Then, the cold-resistant Min pig and the cold-sensitive Wuzhishan (WZS) pig were selected to further investigate their responses to cold stress. As expected, the cold

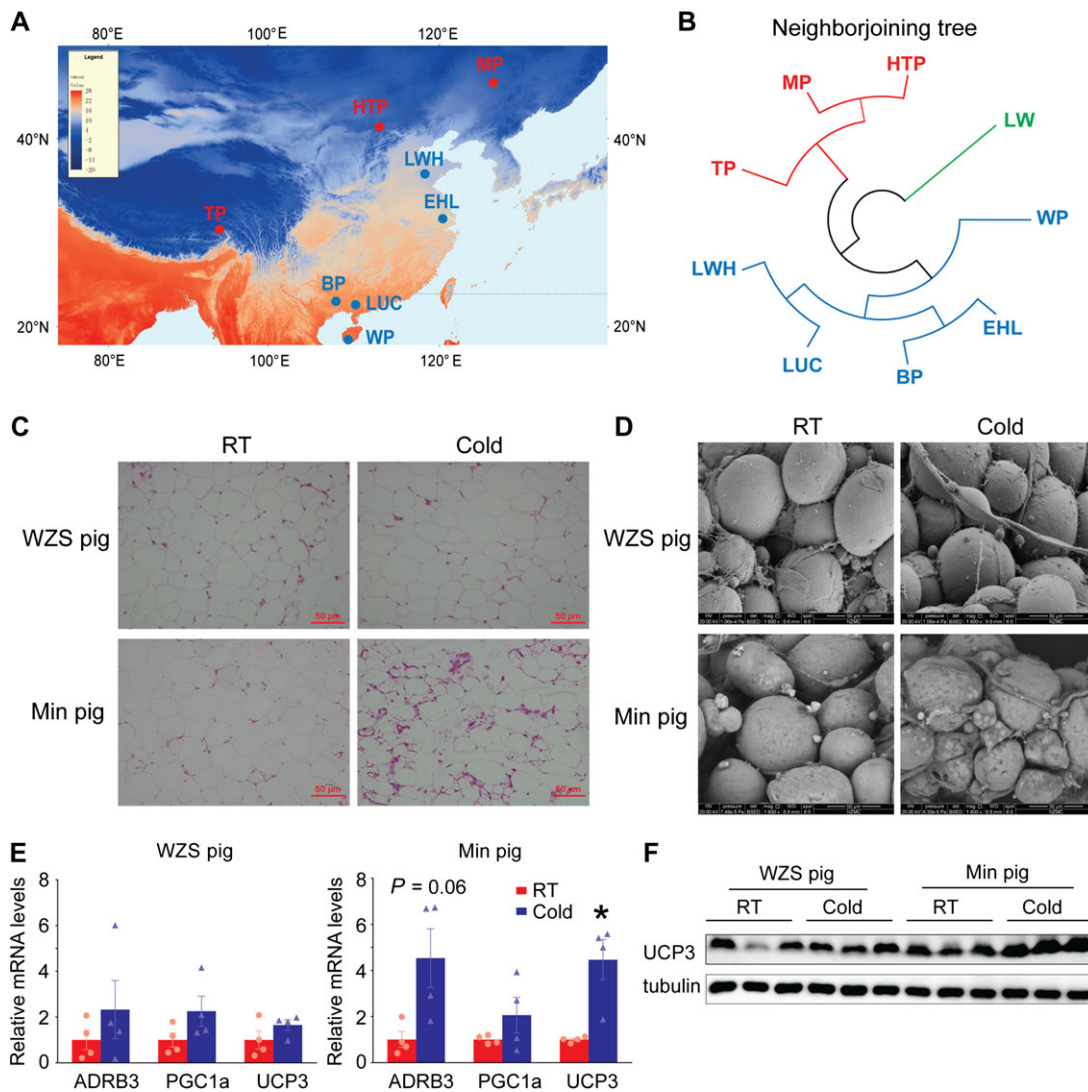


Figure 5 UCP3 might be a key element in the evolution of cold adaption in pig lineages. (A) Geographic locations of pig breeds on a climate map. The map was drawn using annual temperature data from www.worldclim.org. TP, Tibetan pig; BP, Bama pig; MP, Min pig; WP, WZS pig; HTP, Hetao pig; EHL, Erhualian pig; LWH, Laiwu pig; LUC, Luchuan pig. (B) Neighbor joining tree of pig breeds based on the *UCP3* gene (CDS sequences). Different colors represent clusters of subpopulations. In addition to the breeds listed in A, the Large White (LW) pig, a western breed, was also included. (C) Representative H&E staining of subcutaneous fat tissue sections from Min pigs and WZS pigs under RT and cold conditions. (D) Scanning electron micrographs of subcutaneous fat from Min pigs under RT and cold conditions. (E and F) mRNA expression levels of ADRB3, PGC-1 α , and UCP3 (E) and protein levels of UCP3 (F) in subcutaneous fat from Bama pigs and Tibetan pigs under RT and cold conditions. Data are presented as mean \pm SEM ($n = 4$). * $P < 0.05$; data were analyzed with an unpaired t -test.

stimulation-induced formation of beige adipocytes (Figure 5C and D) and induction of ADRB3, PGC-1 α , and UCP3 (Figure 5E and F) were observed only in Min pigs.

Furthermore, the phylogenetic tree constructed using the *UCP3* genomic sequences from different pig breeds could classify the cold-tolerant (groups 1 and 3, 83.3% and 71.4% are cold-tolerant breeds) and cold-sensitive (groups 2 and 4, 85% and 100% are cold-sensitive breeds) pigs. This result further implied that the *UCP3* gene represents a genetic link to cold tolerance in pigs (Supplementary Figure S6).

Discussion

Many studies have established the well-recognized link between the presence of active BAT and NST in mammals (Cannon and Nedergaard, 2004) and the critical role of UCP1 in energy homeostasis (Oelkrug et al., 2015). However, the thermoregulatory ability of pigs has been reported as 'very poor' (Berg et al., 2006), because pigs lost exons 3–5 of *UCP1* in a genetic event ~20 million years ago and appear to lack functional BAT (Trayhurn et al., 1989; Berg et al., 2006). Pigs can maintain their body temperature relatively independently of the ambient temperature, thus allowing them to adapt to various environments. The acquisition of novel physiological mechanisms for body temperature regulation would be important for pig breeds exposed to environments that they were not primarily adapted.

Tibetan pigs are geographically located in cold regions of China and are one of the well-recognized cold-tolerant pig breeds (Li et al., 2013). Consistent with previous reports for cold-sensitive pigs (Trayhurn et al., 1989; Berg et al., 2006; Jastroch and Andersson, 2015), we found that neither classical BAT nor gene expression for the (predicted) deleted UCP1 locus was observed in neonatal Tibetan pigs. Here, we provide novel evidence showing that muscle-independent thermoregulatory ability exists in cold-resistant Tibetan pigs but not in cold-sensitive Bama pigs. Furthermore, in agreement with the emergence of beige adipocytes in cold-challenged mice (Shabalina et al., 2013), beige cells were observed in cold-treated Tibetan pigs, as evidenced by the positive PET signals, morphological characteristics, and upregulated expression of beige adipocyte-related genes. Moreover, beige cells from Tibetan pigs showed profound oxidative capacity compared with those from Bama pigs. Recent studies revealed that enhancing the browning of WAT alone is sufficient to reduce obesity in mice (Cohen et al., 2014). We believe that the activation of beige cells in Tibetan pigs upon acute cold stress plays a critical role in heat balance allowing them to tolerate cold conditions without extensive shivering.

Furthermore, consistent with previous Tibetan wild boar genomic analysis (Li et al., 2013), our deep sequencing data revealed the enrichment of 'lipid metabolism'-related genes (*DHRS4*, *LIPE*, *NR4A3*, *SDR16C5*, *PCK1*, *ABHD5*, *PLIN5*, *PDK4*, etc.) and pathways in Tibetan pigs, which reflects the requirement of evolving energy metabolic genes to protect them against the cold environment. In contrast, 'immune response'-related genes (*PVR*, *THBS1*, *IL1A*, *RSAD2*, *NFIL3*, *DDX60*, etc.) and pathways were enriched in Bama pigs upon cold exposure, which

indicates that the acute response to the external cold stimulation is not primarily concerned with heat generating mechanisms in this tropical pig breed.

Strikingly, upregulation of UCP3 was observed in beige adipocytes from cold-treated Tibetan pigs, which was consistent with previous reports in rodent (Larkin et al., 1997; Nau et al., 2008). Early studies suggested that UCP3 may play a central role in NST, alongside UCP1 (Krauss et al., 2005). UCP3 has been reported to be a possible candidate as an uncoupling protein involved in thermogenesis (Ljubcic et al., 2004; Nabben et al., 2008; Lombardi et al., 2010) and has exhibited uncoupling activity (Gong et al., 1997; Krauss et al., 2002). Loss of UCP3 function specifically in the BAT of hamsters (*Phodopus*) caused impaired NST (Nau et al., 2008). However, the response of the global UCP1^{-/-} mice to cold exposure, which depends exclusively on elevated long-term shivering, strongly supported that in the absence of UCP1, the heat generated from these alternative sources of uncoupling, including UCP3, was unable to substitute heat production at any meaningful level. Therefore, the most recent opinion is that the only significant source of non-shivering thermogenic heat is the uncoupled respiration mediated via UCP1 (Cannon and Nedergaard, 2004; Shabalina et al., 2010).

Our data for pigs challenge this mouse-based orthodoxy by demonstrating that cold-tolerant pigs can thermoregulate and maintain their body temperature even in the absence of UCP1 and blocking shivering or NST. This is linked to significantly enhanced WAT browning and upregulation of UCP3. Moreover, overexpression of UCP3 enhanced the oxidative capacity of beige cells from Tibetan pigs, suggesting the potential thermogenic ability of porcine UCP3. Excitingly, the cold-sensitive and cold-resistant pig breeds could be clearly separated based on the cDNA and genomic sequence of UCP3, suggesting that UCP3-mediated thermogenesis in cold-resistant pig lineages is an adaptation to cold environments. This genetic event would have been the result of interactions between natural and artificial selection during the evolutionary history of the pig. Taken together, we demonstrate here that cold-resistant pig breeds, such as Tibetan pigs and Min pigs, use a novel mechanism that relies on recruited beige cells and UCP3-mediated heat production when they confront cold conditions. The evolution of these mechanisms was probably key in allowing these pig breeds to survive when exposed to unfamiliar cold environments.

This work also has important practical implications. Neonatal mortality of piglets caused by the cold stress at birth is a major concern for the swine industry in cold regions worldwide, because reduced piglet survival rates in such areas cause huge economic losses in pig production (Fainberg et al., 2012). Fully understanding the molecular mechanisms of thermoregulation in cold-resistant pigs might provide a strategy for small molecules and/or genome-editing techniques to reduce cold stress-mediated neonatal mortality, which would improve production efficiency in the pig industry.

In conclusion, our study revealed that cold-resistant pig breeds have evolved a novel mechanism involving UCP3 in beige adipocytes as the primary thermogenic mechanism,

challenging the orthodoxy based on studies of mice that only UCP1 may act as a significant source of thermogenic heat.

Materials and methods

Animals

The pigs used in this study had *ad libitum* access to a commercial pig diet (nutrient levels according to the NRC) and water throughout the experimental period. All experiments involving animals were performed according to the procedures approved by the Institutional Animal Care and Use Committee of the Institute of Zoology, Chinese Academy of Sciences (CAS). Bama miniatures were provided by the pig farm affiliated with the Institute of Animal Science, Chinese Academy of Agricultural Sciences. Tibetan pigs were provided by Beijing Farm Animal Research Center affiliated with the Institute of Zoology, CAS. WZS pigs were purchased from Beijing Grand Life Science & Technology Co., Ltd. Min pigs were purchased from Lanxi Pig Farm in Harbin, China. C57BL/6 mice at 8 weeks of age were purchased from Vital River Laboratory Animal Technology Co., Ltd.

Cold challenge experiment

A cold tolerance test was performed with 5-week-old piglets. Prior to cold exposure, piglets were administered curare (Sigma-Aldrich) at 0.16 mg/kg body weight (Kashimura et al., 1992) or dantrolene (Sigma-Aldrich) at 4 mg/kg body weight (Bal et al., 2012), as previously reported. Saline solution was used as the control. Pigs were visually monitored for 15 min and then placed in a cold chamber (4°C) for up to 4 h with free access to food and water. The status of shivering was monitored during the first half hour of cold treatment. Body temperature was measured using a rectal probe connected to digital thermometer (Yellow Spring Instruments) every 30 min for up to 3 h.

Positron-emission tomography

For all studies in this work, data were acquired using a whole-body PET scanner (Judicious PET L900), which was developed by the Institute of High Energy Physics, CAS. The scanner uses LYSO-based detector blocks with a 70-cm transaxial field-of-view (FOV) and a 21.6-cm axial FOV. According to the National Electrical Manufacturers Association (NEMA) NU 2-2007 procedures, the transverse (axial) spatial resolution FWHMs were measured to be 4.4 (3.9) mm and 5.1 (4.0) mm at 1 and 10 cm off axis, respectively, and the sensitivity average at 0 and 10 cm was 13.2 cps/kBq. The emission projection data were acquired in listmode format and were Fourier re-binned into two-dimensional (2D) sinograms. Images were then reconstructed using the 2D OSEM algorithm (4 iterations and 16 subsets), resulting in $2.0 \times 2.0 \times 1.8$ mm³ voxel size for a $320 \times 320 \times 119$ image volume. The PET images were corrected for detector efficiency, dead-time, decay, photon scatter, and attenuation.

Microscopy

For histological analysis, adipose tissues were fixed in 4% paraformaldehyde, dehydrated overnight in 70% ethanol, and embedded in paraffin. Multiple sections were prepared and

stained with hematoxylin and eosin (H&E). Images were taken with a microscope (DS-R11; Nikon). For scanning electron microscopy, adipose tissues were fixed in 2% (v/v) glutaraldehyde in 100 mM phosphate buffer, pH 7.2, for 12 h at 4°C. The sections were then post-fixed in 1% osmium tetroxide and dehydrated in ascending gradations of ethanol. Samples were critical point dried by using an Automated Critical Point Dryer (Leica EM CPD300) and coated with gold using a Super Cool Sputter Coater (Leica EM SCD050). Sections were then visualized using an Environmental Scanning Electron Microscope (FEI Quanta 450). For TEM, adipose tissues were fixed in 2% (v/v) glutaraldehyde in 100 mM phosphate buffer, pH 7.2, for 12 h at 4°C. The samples were then post-fixed in 1% osmium tetroxide, dehydrated in ascending gradations of ethanol, and embedded in fresh epoxy resin 618. Ultrathin sections (60–80 nm) were cut and stained with lead citrate before being examined on a Phillip CM-120 TEM.

RNA preparation and real-time PCR

Tissues were lysed and homogenized in a TissueLyser (Qiagen), and total RNA was extracted using Trizol reagent (Invitrogen). The quality and the purity of total RNA were tested using a NanoDrop ND-1000 spectrophotometer (Nano Drop) and an Agilent 2100 Bioanalyzer (Agilent). Reverse transcription of 2 µg total RNA was performed with a high-capacity cDNA reverse transcription kit (Promega). Real-time PCR was performed in triplicates with SYBR Green Master Mix (Promega). The PCR reactions were run in triplicates for each sample and were quantified using an ABI Prism 7500 real-time PCR instrument (Applied Biosystems). The relative expression level of genes was calculated using the $2^{-\Delta\Delta CT}$ method. The primer sequences are listed in Supplementary Table S2.

Deep sequencing

Sequencing library preparation and RNA-seq were conducted at Berry Genomics. Paired-end (PE) libraries for sequencing were prepared according to the Illumina PE library preparation protocol (Illumina). The qualified libraries were sequenced on an Illumina HiSeq 2000 sequencing platform to generate 2×100 PE reads. To map the reads, reads in fastq format were split based on the index, and the adapters were trimmed out. A Trimmomatic program was used to detect adapter contamination and remove sequencing reads with low-quality bases with the following command ‘illumina_adapters.fa:2:30:10 LEADING:3 TRAILING:3 SLIDINGWINDOW:4:15 MINLEN:50’. The remaining qualified reads (regarded as clean reads) were then aligned to the pig built 10.2 reference sequence using TopHat software with default parameters. The BAM files (generated from TopHat) that contained the read alignments were then used to evaluate gene expression levels by fragments per kilobase of exon per million fragments mapped (FPKM) values using Cufflinks software. Our RNA-seq data are deposited in the GenBank BioProject section, with the accession number PRJNA339666. The raw sequencing reads have been submitted to the short read archive (SRA) database, with the assigned accession number SRP082487.

DEG identification

To measure the expression level changes, the number of uniquely mapped reads assigned to each gene in the pig genome was first counted using the featureCounts package according to the gene annotation file for pigs (*Sus_scrofa*. *Sscrofa10.2.83.gtf*), which was downloaded from the Ensembl genome browser. edgeR software that uses the raw read counts as input, and then used to identify the differentially expressed transcripts in different groups using a threshold value of FDR < 0.05 and an absolute fold change ≥ 2 .

Clustering analysis and GO analysis

The heatmap.2 function in gplots was used to perform hierarchical clustering of DEGs with a Euclidean distance metric and to generate heat maps to represent the gene clusters showing similar expression patterns. GO enrichment analysis of upregulated and downregulated genes was performed using the 'g:Profiler' enrichment analysis tool (<http://biit.cs.ut.ee/gprofiler/>). The GO terms with *P*-values (enrichment score) < 0.05 were regarded as 'statistically significant' and were highlighted in the heat maps.

Porcine primary pre-adipocyte isolation and in vitro differentiation

Adipose tissues were harvested from 1-week-old piglets, minced, and digested with 2 mg/ml collagenase type I (Sigma) in Dulbecco's modified Eagle's medium (DMEM)/F12 (Gibco) plus 1% fatty acid-free bovine serum albumin (BSA) (Sigma) for 60 min at 37°C. SVF cells were collected with a cell strainer (70 μ m diameter) and then plated and grown in DMEM/F12 supplemented with 10% fetal bovine serum (FBS) (Sigma) and 1% penicillin–streptomycin. For browning differentiation, cells were grown to confluence and then treated with human BAT induction medium (DMEM/H medium containing 0.5 mM isobutylmethylxanthine, 0.1 μ M dexamethasone, 0.5 μ M human insulin (Sigma), 2 nM T3, 30 μ M indomethacin, 17 μ M pantothenate, 33 μ M biotin, 1 μ M rosiglitazone, and 2% FBS) for 8 days. The induction medium was changed every 2 days. For white adipocyte differentiation, cells were grown until confluence and then treated with human WAT induction medium (DMEM/H medium containing 0.25 mM isobutylmethylxanthine, 0.1 μ M dexamethasone, 66 nM human insulin, 17 μ M pantothenate, 33 μ M biotin, 20 mM HEPES, pH 7.4, and 0.5% FBS) for 5 days. On Day 5, half of the induction medium was removed, and the same volume of human WAT mature medium (DMEM/H medium containing 0.1 μ M dexamethasone, 66 nM human insulin, 17 μ M pantothenate, 33 μ M biotin, 20 mM HEPES, pH 7.4, and 10% FBS) was added. On Day 6, the cells were switched to pure human WAT maturation medium and cultured for 2 days. On Day 8, the fully differentiated adipocytes were used for all the following experiments.

Western blotting

Equal amounts of protein from tissues or cell lysates were fractionated using 12% SDS-PAGE gels and transferred onto polyvinylidene difluoride membranes. The membranes were blocked with

blocking buffer (5% fat-free milk) for 1 h at room temperature and incubated in blocking buffer at 4°C overnight with the following antibodies: anti-UCP3 (Abcam, ab3477), anti-OXPHOS (Abcam), anti-PGC1 α (Abcam), anti-CD137 (Bioss), anti-DIO2 (Santa Cruz Biotech), anti-PRDM16 (R&D), and anti-tubulin (Santa Cruz Biotech). The membranes were incubated with HRP-conjugated secondary antibodies for 1 h at room temperature, and all signals were visualized and analyzed with densitometric scanning (Image Quant TL7.0, GE Healthcare Bio-Sciences AB).

Bioenergetic profiling

Pig primary subcutaneous adipocytes were seeded into gelatin-coated XF24 culture microplates (Seahorse Bioscience) and cultured in DMEM/F12 with 10% FBS and antibiotics (100 units/ml of penicillin and 100 μ g/ml of streptomycin) overnight at 37°C in an atmosphere of 5% CO₂. Next day, the cells were cultured in differentiation medium. On Day 8, the O₂ consumption was measured with a Seahorse Bioscience XF24-3 extracellular flux analyzer. To measure OCR independent of oxidative phosphorylation, 1 μ M oligomycin was added to cells. Subsequently, 0.5 μ M carbonyl cyanide-*p*-trifluoromethoxyphenylhydrazone and 2 μ M respiratory chain inhibitor rotenone were added to measure the maximal respiration and basal non-mitochondrial respiration rates. The means and standard error of the mean (SEM) from three independent experiments are shown. Statistical comparisons were made using Student's *t*-test.

Mitochondrial copy number determination

Total DNA (genomic and mtDNA) was isolated from adipose tissues and adipocytes using the QIAamp DNA Mini kit (Qiagen) according to the manufacturer's instructions. The DNA concentration was assessed using a Nanodrop 2000 (Thermo Scientific). The mtDNA copy number relative to the genomic DNA content was quantitatively analyzed using an ABI Prism ViiA7 real-time PCR instrument (Applied Biosystems). The COX-II and β -globin primers were as follows: COX-II: forward GGC TTACCTTCCAAGTAGG, reverse AGGTGTGATCGTAAAGTGTAG; β -globin: forward GGGGTGAAAAGAGCGCAAG, reverse CAGGTTGG TATCCAGGGCTTCA.

Nucleofection

Primary cells derived from the subcutaneous fat of Tibetan pigs were transfected with vectors expressing UCP3 or shRNA for UCP3 with the nucleofection method.

Statistical analysis

Comparisons between groups were made with one-way ANOVA with Tukey's *post hoc* test or Student's two-sample *t*-test. A between-group difference of *P* < 0.05 was considered significant.

Supplementary material

Supplementary material is available at *Journal of Molecular Cell Biology* online.

Acknowledgements

We are grateful to members of Zhao, Jin, and Wang laboratories for helpful discussions, to P. Chai, S. Liu, H. Tang, and C. Wei from the Institute of High Energy Physics, CAS and Beijing Engineering Research Center of Radiographic Techniques and Equipment for their great help with the PET scan experiments and analysis. The genomic UCP3 sequences were kindly provided by Dr J. Ren from Jiangxi Agricultural University.

Funding

This study was supported by the Strategic Priority Research Program of CAS (XDB13030000 and XDA08010304), the National Transgenic Project of China (2016ZX08009003-006-007), the National Basic Research Program of China (973 Program, 2015CB943100), the Agricultural Science and Technology Innovation Program (ASTIP-IAS05), and the National Natural Science Foundation of China (31402045). Y.W. was supported by the Elite Youth Program of the Chinese Academy of Agricultural Sciences.

Conflict of interest: none declared.

References

- Alan, L., Smolkova, K., Kronusova, E., et al. (2009). Absolute levels of transcripts for mitochondrial uncoupling proteins UCP2, UCP3, UCP4, and UCP5 show different patterns in rat and mice tissues. *J. Bioenerg. Biomembr.* *41*, 71–78.
- Attig, L., Djiane, J., Gertler, A., et al. (2008). Study of hypothalamic leptin receptor expression in low-birth-weight piglets and effects of leptin supplementation on neonatal growth and development. *Am. J. Physiol. Endocrinol. Metab.* *295*, E1117–E1125.
- Bal, N.C., Maurya, S.K., Sopariwala, D.H., et al. (2012). Sarcolipin is a newly identified regulator of muscle-based thermogenesis in mammals. *Nat. Med.* *18*, 1575–1579.
- Berg, F., Gustafson, U., and Andersson, L. (2006). The uncoupling protein 1 gene (UCP1) is disrupted in the pig lineage: a genetic explanation for poor thermoregulation in piglets. *PLoS Genet.* *2*, e129.
- Bowman, W.C. (2006). Neuromuscular block. *Br. J. Pharmacol.* *147*(Suppl 1), S277–S286.
- Cannon, B., and Nedergaard, J. (2004). Brown adipose tissue: function and physiological significance. *Physiol. Rev.* *84*, 277–359.
- Cannon, B., and Nedergaard, J. (2010). Metabolic consequences of the presence or absence of the thermogenic capacity of brown adipose tissue in mice (and probably in humans). *Int. J. Obes.* *34*(Suppl 1), S7–S16.
- Cohen, P., Levy, J.D., Zhang, Y., et al. (2014). Ablation of PRDM16 and beige adipose causes metabolic dysfunction and a subcutaneous to visceral fat switch. *Cell* *156*, 304–316.
- Cypess, A.M., Lehman, S., Williams, G., et al. (2009). Identification and importance of brown adipose tissue in adult humans. *N. Engl. J. Med.* *360*, 1509–1517.
- Dempersmier, J., Sambeat, A., Gulyaeva, O., et al. (2015). Cold-inducible Zfp516 activates UCP1 transcription to promote browning of white fat and development of brown fat. *Mol. Cell* *57*, 235–246.
- Divakaruni, A.S., and Brand, M.D. (2011). The regulation and physiology of mitochondrial proton leak. *Physiology* *26*, 192–205.
- Fainberg, H.P., Bodley, K., Bacardit, J., et al. (2012). Reduced neonatal mortality in Meishan piglets: a role for hepatic fatty acids? *PLoS One* *7*, e49101.
- Golozubova, V., Hohtola, E., Matthias, A., et al. (2001). Only UCP1 can mediate adaptive nonshivering thermogenesis in the cold. *FASEB J.* *15*, 2048–2050.
- Gong, D.W., He, Y., Karas, M., et al. (1997). Uncoupling protein-3 is a mediator of thermogenesis regulated by thyroid hormone, beta3-adrenergic agonists, and leptin. *J. Biol. Chem.* *272*, 24129–24132.
- Gonzalez-Barrero, M.M., Fleury, C., Jimenez, M.A., et al. (1999). Structural and functional study of a conserved region in the uncoupling protein UCP1: the three matrix loops are involved in the control of transport. *J. Mol. Biol.* *292*, 137–149.
- Harper, M.E., Dent, R., Monemdjou, S., et al. (2002). Decreased mitochondrial proton leak and reduced expression of uncoupling protein 3 in skeletal muscle of obese diet-resistant women. *Diabetes* *51*, 2459–2466.
- Ishibashi, J., and Seale, P. (2010). Medicine. Beige can be slimming. *Science* *328*, 1113–1114.
- Jastroch, M., and Andersson, L. (2015). When pigs fly, UCP1 makes heat. *Mol. Metab.* *4*, 359–362.
- Jezek, P., and Garlid, K.D. (1998). Mammalian mitochondrial uncoupling proteins. *Int. J. Biochem. Cell Biol.* *30*, 1163–1168.
- Kashimura, O., Sakai, A., Yanagidaira, Y., et al. (1992). Thermogenesis induced by inhibition of shivering during cold exposure in exercise-trained rats. *Aviat. Space Environ. Med.* *63*, 1082–1086.
- Keipert, S., and Jastroch, M. (2014). Brite/beige fat and UCP1—is it thermogenesis? *Biochim. Biophys. Acta* *1837*, 1075–1082.
- Klingenberg, M. (2010). Wanderings in bioenergetics and biomembranes. *Biochim. Biophys. Acta* *1797*, 579–594.
- Klingenspor, M., Fromme, T., Hughes, D.A., Jr, et al. (2008). An ancient look at UCP1. *Biochim. Biophys. Acta* *1777*, 637–641.
- Krauss, S., Zhang, C.Y., and Lowell, B.B. (2002). A significant portion of mitochondrial proton leak in intact thymocytes depends on expression of UCP2. *Proc. Natl Acad. Sci. USA* *99*, 118–122.
- Krauss, S., Zhang, C.Y., and Lowell, B.B. (2005). The mitochondrial uncoupling-protein homologues. *Nat. Rev. Mol. Cell Biol.* *6*, 248–261.
- Larkin, S., Mull, E., Miao, W., et al. (1997). Regulation of the third member of the uncoupling protein family, UCP3, by cold and thyroid hormone. *Biochem. Biophys. Res. Commun.* *240*, 222–227.
- Li, M., Tian, S., Jin, L., et al. (2013). Genomic analyses identify distinct patterns of selection in domesticated pigs and Tibetan wild boars. *Nat. Genet.* *45*, 1431–1438.
- Ljubicic, V., Adhietty, P.J., and Hood, D.A. (2004). Role of UCP3 in state 4 respiration during contractile activity-induced mitochondrial biogenesis. *J. Appl. Physiol.* *97*, 976–983.
- Lombardi, A., Busiello, R.A., Napolitano, L., et al. (2010). UCP3 translocates lipid hydroperoxide and mediates lipid hydroperoxide-dependent mitochondrial uncoupling. *J. Biol. Chem.* *285*, 16599–16605.
- Meister, B., Fried, G., Hokfelt, T., et al. (1988). Immunohistochemical evidence for the existence of a dopamine- and cyclic AMP-regulated phosphoprotein (DARPP-32) in brown adipose tissue of pigs. *Proc. Natl Acad. Sci. USA* *85*, 8713–8716.
- Mostyn, A., Attig, L., Larcher, T., et al. (2014). UCP1 is present in porcine adipose tissue and is responsive to postnatal leptin. *J. Endocrinol.* *223*, M31–M38.
- Nabben, M., Hoeks, J., Briede, J.J., et al. (2008). The effect of UCP3 overexpression on mitochondrial ROS production in skeletal muscle of young versus aged mice. *FEBS Lett.* *582*, 4147–4152.
- Nau, K., Fromme, T., Meyer, C.W., et al. (2008). Brown adipose tissue specific lack of uncoupling protein 3 is associated with impaired cold tolerance and reduced transcript levels of metabolic genes. *J. Comp. Physiol. B* *178*, 269–277.
- Oelkrug, R., Polymeropoulos, E.T., and Jastroch, M. (2015). Brown adipose tissue: physiological function and evolutionary significance. *J. Comp. Physiol. B* *185*, 587–606.
- Puigserver, P., Wu, Z., Park, C.W., et al. (1998). A cold-inducible coactivator of nuclear receptors linked to adaptive thermogenesis. *Cell* *92*, 829–839.
- Schrauwen, P., and Hesselink, M. (2002). UCP2 and UCP3 in muscle controlling body metabolism. *J. Exp. Biol.* *205*, 2275–2285.
- Schulz, T.J., Huang, P., Huang, T.L., et al. (2013). Brown-fat paucity due to impaired BMP signalling induces compensatory browning of white fat. *Nature* *495*, 379–383.

- Shabalina, I.G., Hoeks, J., Kramarova, T.V., et al. (2010). Cold tolerance of UCP1-ablated mice: a skeletal muscle mitochondria switch toward lipid oxidation with marked UCP3 up-regulation not associated with increased basal, fatty acid- or ROS-induced uncoupling or enhanced GDP effects. *Biochim. Biophys. Acta* 1797, 968–980.
- Shabalina, I.G., Petrovic, N., de Jong, J.M., et al. (2013). UCP1 in brite/beige adipose tissue mitochondria is functionally thermogenic. *Cell Rep.* 5, 1196–1203.
- Sokolova, I.M., and Sokolov, E.P. (2005). Evolution of mitochondrial uncoupling proteins: novel invertebrate UCP homologues suggest early evolutionary divergence of the UCP family. *FEBS Lett.* 579, 313–317.
- Symonds, M.E., and Lomax, M.A. (1992). Maternal and environmental influences on thermoregulation in the neonate. *Proc. Nutr. Soc.* 51, 165–172.
- Trayhurn, P., Temple, N.J., and Van Aerde, J. (1989). Evidence from immunoblotting studies on uncoupling protein that brown adipose tissue is not present in the domestic pig. *Can. J. Physiol. Pharmacol.* 67, 1480–1485.
- Ukropec, J., Anunciado, R.P., Ravussin, Y., et al. (2006). UCP1-independent thermogenesis in white adipose tissue of cold-acclimated Ucp1^{-/-} mice. *J. Biol. Chem.* 281, 31894–31908.
- Virtanen, K.A., Lidell, M.E., Orava, J., et al. (2009). Functional brown adipose tissue in healthy adults. *N. Engl. J. Med.* 360, 1518–1525.
- Wang, R., Zhong, X., Meng, X., et al. (2011). Localization of the dantrolene-binding sequence near the FK506-binding protein-binding site in the three-dimensional structure of the ryanodine receptor. *J. Biol. Chem.* 286, 12202–12212.
- Wu, J., Bostrom, P., Sparks, L.M., et al. (2012). Beige adipocytes are a distinct type of thermogenic fat cell in mouse and human. *Cell* 150, 366–376.